M. M. Moghadam[*]
M.Sc. Student

Sh. Zangeneh[†]
Assistant Professor

S. Rasaee[‡]
Assistant Professor

M. Mojtahedi[§]
Associate Professor

The Johnson-cook Constitutive Equation for Compression Behavior of the New Piston Aluminum Alloys at High Temperatures

New alloys of aluminum piston alloy made by adding more nickel to their usual composition. Bulk-forming of new alloys at ambient temperature by conventional methods is not possible. Therefore, the hot-compression deformation behavior of these alloys has been studied in this study. Based on the true stress-strain graphs obtained from the experiments, the constitutive model proposed for these alloys based on the Johnson-Cook model. Then this model is improved by considering the coupled effects of the parameters. The accuracy of the proposed models has been investigated using appropriate statistical analysis, and as a result, the accuracy of the presented models has been confirmed. The modified model, compared to original model, in addition to the higher accuracy, can predict the trend of changes in flow stress. The study of variations of the model coefficients shows that with an increasing nickel content in the alloy composition, the strength and the flow stress of the alloys increased intensely at all temperatures and strain rates. Also, by increasing the amount of nickel, the effect of the strain rate on flow stress is reduced.

1 Introduction

By consideration of the complex working conditions of pistons, they must be made from alloys, which have good strength at temperature ranges of 350 to 400°C [1]. In addition to high-temperature resistance, low Coefficient of Thermal Expansion (CTE) and low Thermal Conductivity (TC) are considered as critical physical properties for the piston alloys because TC and CTE can play as crucial roles over efficient life-span of components [2]. Based on all specific properties required, Al-Si alloys are used in the production of pistons and widely use in the aerospace and automotive industries as well [3]. In general, Al-Si alloys are commonly

---

[*]MSc Student, Department of Materials and Textile Engineering, Faculty of Engineering, Razi University, Kermanshah, Iran, mehdimirzaeimoghadam@gmail.com

[†] Assistant Professor, Department of Materials and Textile Engineering, Faculty of Engineering, Razi University, Kermanshah, Iran, shzangeneh@razi.ac.ir

[‡] Corresponding author, Assistant Professor, Department of Mechanical Engineering, Faculty of Engineering, Kermanshah University of Technology, Kermanshah, Iran, rasaee@kut.ac.ir

[§] Assistant Professor, Department of Materials and Textile Engineering, Faculty of Engineering, Razi University, Kermanshah, Iran, M.mojtahedi@razi.ac.ir

used in this industry by reason of their excellent abrasion corrosion resistance, high strength to weight ratio, good flexibility, and more importantly, resistance against high temperatures operation.

At the operation temperature of piston alloys, the ultimate tensile strengths and yield stress tend to decrease due to the smooth movement of dislocations as well as the occurrence of recovery and dynamic recrystallization [3]. As a result, the strength used in high temperatures is one of the critical criteria in the production and design of pistons. Alloying, using a large number of alloying elements such as nickel, strontium, copper, is one of the most common methods to improve mechanical properties, especially the high-temperature strength of such alloys by intermetallic phase's formation and postponing recovery and dynamic recrystallization [2]. Nickel is known as the most productive element to improve high-temperature properties of piston alloys due to the intermetallic phases that it forms [4]. Li et al. have reported that among such phases, ε-Al_3Ni, δ-Al_3CuNi, and γ-Al_7Cu_4Ni intermetallic phases have the highest role in improving the high-temperature properties of piston alloys [5]. Similarly, Stadler et al. reported that by addition of 2.1% Ni to Al-12%Si, high-temperature strength of the alloy is improved from 90MPa (in 0%Ni) to 120MPa (in 2.1%Ni) at 250°C [6]. These studies confirm that the addition of nickel can have a beneficial change in improving the mechanical properties of Al-Si alloy, especially at high temperatures, that was the reason for choosing this research topic. Mirzaee-Moghadam et al. [7] By investigating the effect of adding nickel element in different amounts ranging from 0.8% to 3.5% and examining their deformation behavior showed that with increasing the amount of nickel element in piston alloy - due to the formation of stable intermetallic phases at high temperatures, good strength High temperature improves the alloy as well as abrasion and corrosion resistance. Understanding how materials behave in different conditions such as high temperatures, different strain rates, and the process of flow stress change in these conditions by applying strain is essential information to ensure the correct performance of the component and also to design the manufacturing process. Constitutive equations mathematically express the relationship between flow stress, strain, strain rate, and temperature. Johnson-cook (JC) model, which is one of the common types of constitutive equations that presents the relationship between several variables such as flow stress, effective strain and, its rate as well as the temperature of various deformation levels [8]; this relationship could be linear or nonlinear. The JC mathematical equation is consisting of a set of constants and variables that each of the constants indicates the sensitivity of the flow stress to a particular process during deformation, for example, showing the strain hardening or softening caused by increasing temperature. In the constitutive equations, in addition to obtaining a mathematical equation that can be useful for modeling a variety of forming processes, it also provides numerical and quantitative information on the behavior of the alloys such as work-hardening and softening. Also, the JC model is desirable because of its availability in finite element engineering software such as the Abaqus. This model has been applied to describe the hot-deformation behavior of aluminum alloys [9, 10], and other alloys [11-14].

Samantaray et al. [15] studied the proficiency of the JC model to study the deformation behavior of modified 9Cr-1Mo steel at high temperatures and strain rates range of 0.001–1 s^{-1} and examined the accuracy of this model compared to other models. Hou and Wang [16] used the JC model to study the flow stress of the Mg–Gd–Y alloy in a wide range of temperatures; modifying the original model, they could improve the accuracy. Lin et al. [13] suggested a model based on the JC model to describe behaviors of high strength steel in high temperature. He et al. [11] in a study, studied the deformation of 20CrMo alloy steel at high temperatures and compared different constitutive models, and found JC model useful to predict flow stress at high temperatures. Abbasi-Bani et al. [9] by an extensive investigation on the ability of JC and Arrhenius constitutive studied the hot deformation flow stress of Mg–6Al–1Zn alloy, and adopted the Cook model as a simple, practical, and accurately accepted the model. Chen et al.

[17] modeled the deformation of homogenized 6026 aluminum alloy at elevated temperatures using the JC model and examined the capabilities, and particularly the weaknesses of this model. Immanuel and Panigrahi [9] studied the high-temperature deformation of ultrafine-grained A356 material and extracted the JC model for this material. Rasaee and Mirzaei [18] proposed a constitutive equation by using the JC model for Al2024 at a wide range of temperatures and strain rate. One of the methods of piston forming is the forging technique, and it can be simulated to ensure that the process is right and acceptable. The crucial requirements of any simulation are the detailed information of how the material behaves in the deformation condition and the availability of the proper mathematical model.

In this study, the concentration of Ni was increased from 0.8 to 2.6% in the Al–Si alloy to investigate hot deformation behaviors by using of hot compression test in different temperatures and strain rates. Furthermore, a mathematical model was extracted using the Johnson-Cook (JC) model which could be beneficial for those working in the car manufacturing industry.

2   Experimental procedure

Aluminum 4032 alloys are used to make pistons, so they are called aluminum piston alloys. These series of alloys, which are a subset of aluminum-silicon alloys, typically contain 0.8% nickel. It is expected that by increasing nickel content up to 2.6%, its mechanical properties, as well as its hot deformation behavior, will be different with respect to base alloy; various studies were performed. to understand the changes in the physical and mechanical properties of this alloy, including abrasion, corrosion and hardness and the list goes on, due to the addition of nickel and its effect, however in this paper only the study of the extraction of constitutive equations for these alloys in high-temperature deformation has been studied [7]. Table (1) shows the chemical composition of the alloys.

To investigate the thermo mechanical behavior of the alloys, a hot compression test has been selected. Due to the lack of necking during the pressure test and, consequently the lack of relative limitation in applied strain, this method is used in many studies to investigate deformation and to model the thermomechanical process. Cylindrical specimens of 8 mm in diameter and 12 mm in height were cut and prepared by machining according to the ASTM E209 standard (Figure 1). The samples were heat-treated based on the homogenized treatment process at 550°C for 4h [19]. To investigate the mechanical behavior of the alloys at elevated temperature, the hot pressure test at the strain rate of 0.001-1 s^{-1}, and the temperature range from 400 to 550 °C, with steps of 50 °C between temperatures, up to a strain of 0.6 were performed.

A combination of graphite powder and refractory grease has been used to reduce friction, and due to the insignificance of the barrel phenomenon, the friction in the process has been neglected. At first, by the rate of 10K/s the sample was heated to the desired deformation temperature, and kept at this temperature for 300s for the same temperature throughout the sample, and then hot deformation was performed.

The Al4032 alloy is a subset of the Al-Si alloys, which contains α-Al, eutectic Si as main phases along with different intermetallic phases. The structure of the hypo-eutectic alloys, (% wt) Si<12.6, includes the primary aluminum and eutectic Al-Si dendrites, and in the microscopic structure of hyper-eutectic alloys, (% wt) Si>12.6, consists of the primary silicon and the

Table 1 The chemical composition of the alloys

	%Wt						
Allo	Mn	Fe	Mg	Ni	Cu	Si	Al
Base Alloy	0.07	0.1	0.7	0.81	3.1	12.6	Balance
Modified Alloy (2% Ni)	0.06	0.1	0.68	2.01	3.1	12.58	Balance
Modified Alloy (2.6% Ni)	0.07	0.09	0.68	2.61	3.1	12.57	Balance

eutectic composition, as shown in Figure (2). The addition of nickel to this alloy system results in the formation of intermetallic phases, which can improve the mechanical properties of these alloys at high temperatures which were also observed in the results of this study. Figure (2) shows the primary microstructures of the investigated alloys.

Due to the chemical composition and microstructure of the alloys, it is not possible to use cold deformation process due to cracking and fracture of the specimens during deformation, so they are formed by the deformation process at high temperature. According to preliminary studies, the deformation temperature range was considered to be 400-550 during hot pressure test because at temperatures less than 400°C, the samples were not capable of severe plastic deformation at high strains because of the cracking and at temperatures above 550°C, the specimens lose their deformation ability due to local melting.

The aim of this research is to study the process of hot deformation of a set of piston aluminum alloys to derive the equation governing its behavior during high-temperature deformation based on the Johnson-Cook model. This set of alloys is obtained by varying the amount of nickel in the composition. These alloys are used to make pistons mainly using the forging method, and modeling of forging processes is a typical process to ensure this process is done correctly. Understanding the mathematical behavioral equation of materials is essential for numerical modeling of high-precision molding processes. Therefore, extracting constitutive equation is necessary and valuable. It should also be noted that the metallurgical study of the manufacturing process of the new alloys and the effect of nickel on the microstructure of the new alloys was not the purpose of this study and is therefore not discussed in this article.
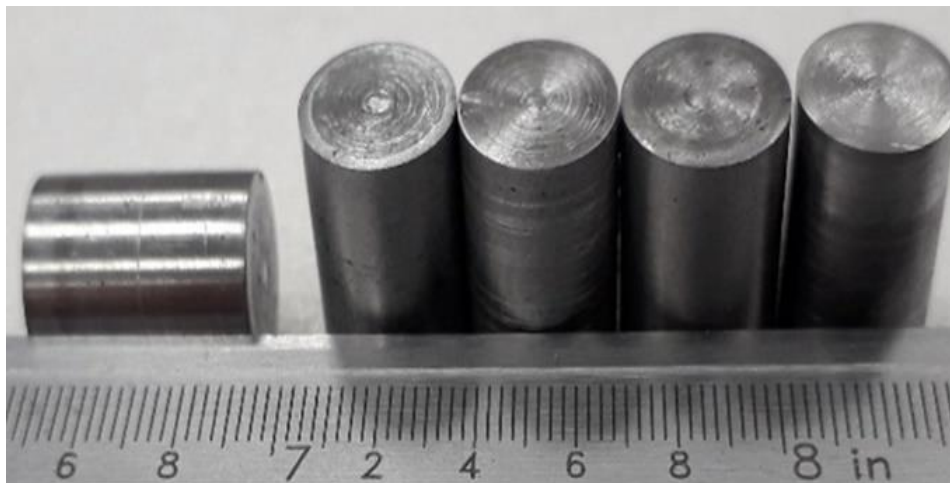

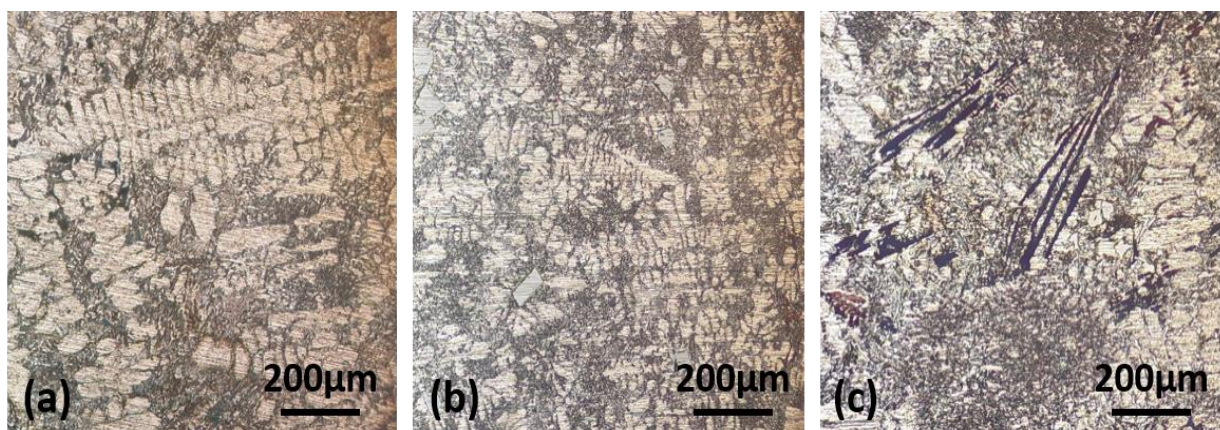**Figure 1** The cylindrical samples for high-temperature compression test.

Figure 2 The initial microstructure of the alloys: a) Al-Si-0.8% Ni, b) Al-Si-2% Ni, c) Al-Si-2.6% Ni.

3   Results

Piston alloys with different Ni contents were hot-deformed to obtain true stress-strain curves (Figure 3, Figure 4 and Figure 5). The dominant mechanism during the hot deformation in these alloys is the dynamic-recovery or recrystallization that can be observed in different parts of the true stress-strain curves of these alloys. As observed from the curves, the flow stress increases sharply with strain at the early stage of hot deformation, which could be due to work hardening as a result of dislocation density increasing. After the early stages, peak stress emerges, and then the flow stress stays nearly constant. There is a tendency for dynamic softening to occur during hot deformation, which is against work hardening. Thus the work hardening and increasing the flow stress cannot continue indefinitely. Due to a dynamic equilibrium between work hardening and dynamic softening, the flow stress gets steady. High stacking fault energy (SFE) is the mechanism of the dynamic recovery and softening of aluminum alloys. To show whether dynamic recrystallization occurs, precise microstructural observation needs to be investigated on the deformed samples [20]. Added to this, it is clear that as temperature increases by severe thermal activation processes, the peak stress decreases. The peak stress, increase as the strain rate increases, which might be due to dislocation generation and multiplication.

In modeling of the materials behavior, the aim is to find a mathematical function that can explain how the flow stress depends on the strain, strain rate, and temperature. Johnson-Cook's constitutive equation is a reasonably simple behavioral equation for simulating forming processes that are used for a wide range of temperature and strain rates. The standard mathematical function of this model is as follow:

$$\sigma = (A + B\varepsilon^n)(1 + C \ln\dot{\varepsilon}^*)(1 - T^{*^m}) \tag{1}$$

In this equation, B is the strain hardening coefficient, n is the work hardening power, and C, and m are the materials constant which are called the strain hardening rate coefficient and heat softening power, respectively. The constants of this equation, although are assumed to be constant and fixed in its standard form, the possibility of the dependence of these constants on other parameters, such as strain, can also be examined and worthwhile.
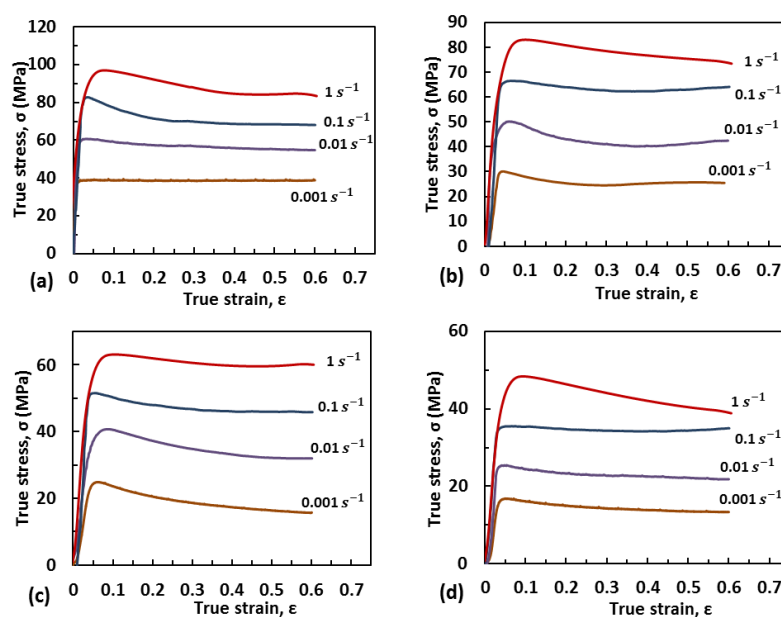

Figure 3 The true stress–strain curves of Al-Si-0.8% Ni with various strain rates and at the deformation temperatures of a) 673K, b) 723K, c) 773K and d) 823K.
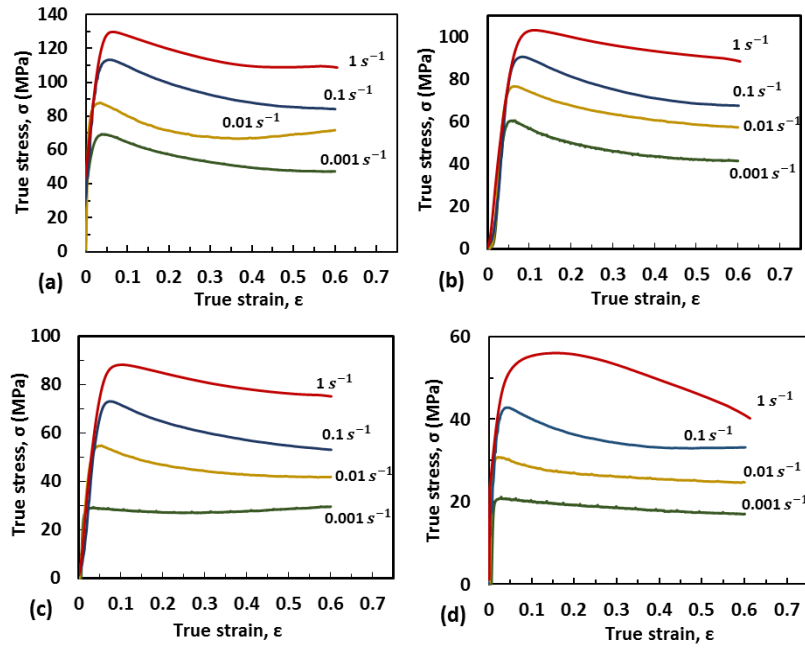
Figure 4 The true stress–strain curves of Al-Si-2% Ni with various strain rates and at the deformation temperatures of a) 673K, b) 723K, c) 773K and d) 823K.
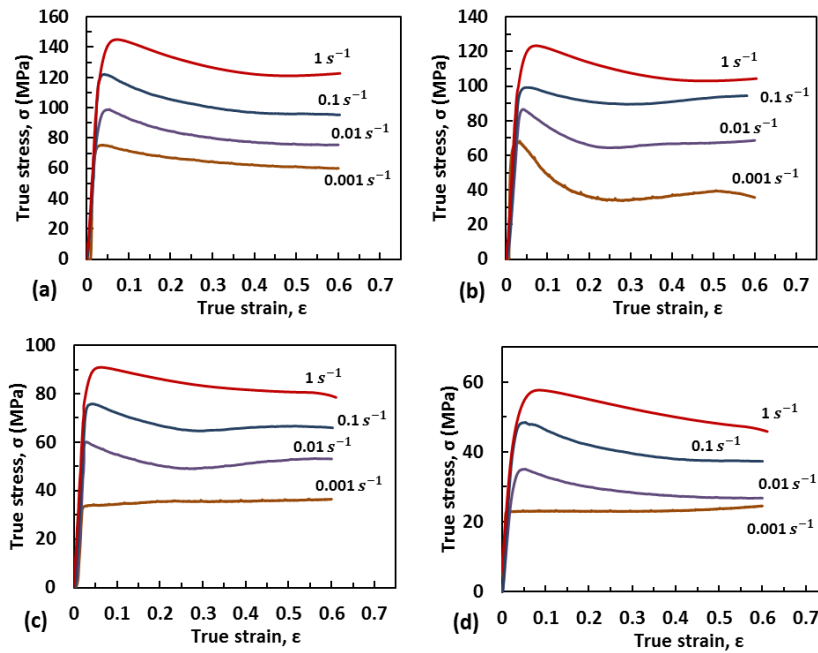

Figure 5 The true stress–strain curves of Al-Si-2.6% Ni with various strain rates and at the deformation temperatures of a) 673K, b) 723K, c) 773K and d) 823K.

3.1   The standard Johnson-Cook model

At the reference strain rate and temperature, the standard equation is transformed as follows that A is the yield stress of the alloy at a reference condition, which is shown in table (2); The values in the table show that as the percentage of nickel in the alloy composition increased, the value of the parameter A as well as the strength of the alloy increased. Therefore, increasing the percentage of nickel can increase the strength, which is a good change for the use of the alloys.
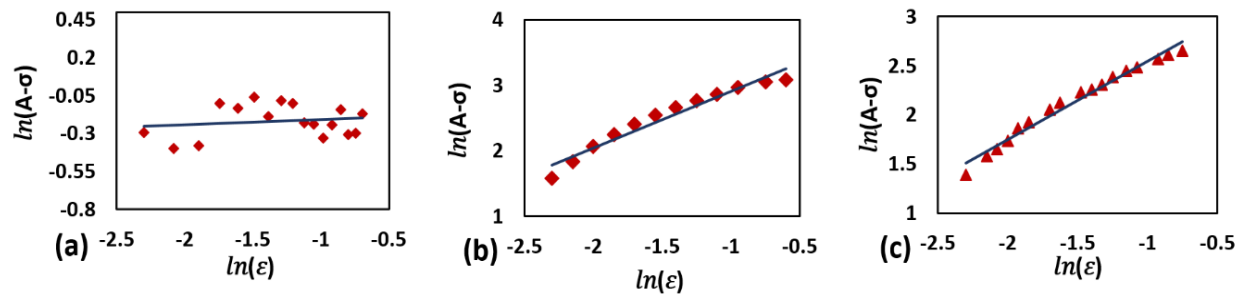
$$\sigma = (A + B\varepsilon^{n}) \qquad\qquad (2)$$

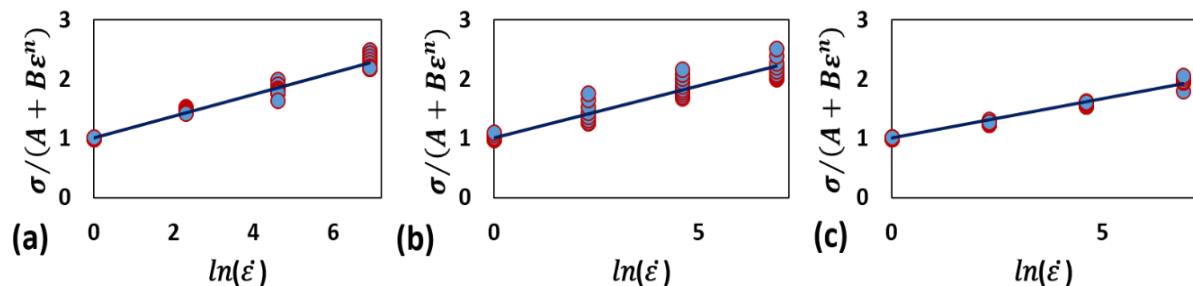**Table 2** The A values for alloys with different weight percentages of nickel

ALLOY	A (MPa)
A (Al-Si-0.8% Ni)	39.42
B (Al-Si-2% Ni)	69.43
C (Al-Si-2.6% Ni)	75.36

Table 3 The n and B values for alloys with different weight percentages of nickel

Alloy	n	B (MPA)
A (Al-Si-0.8% Ni)	0.07	-0.86
B (Al-Si-2% Ni)	0.82	-42.62
C (Al-Si-2.6% Ni)	0.7	-24.49

Figure 6 The curve of $ln(A - \sigma) - ln\,\varepsilon$: a) 0.8% Ni, b)2% Ni, and c) 2.6% Ni.

Table 4 The C values for alloys with different weight percentages of nickel

Alloy	C
Al-Si-0.8% Ni	0.1844
Al-Si-2% Ni	0.1768
Al-Si-2.6% Ni	0.1331

Figure 7 The curve of $\frac{\sigma}{A+B\varepsilon^n} - ln\dot\varepsilon^*$: a) 0.8% Ni, b)2% Ni and c) 2.6% Ni.

Integrating from the sides of the Eq. (2), the values of B and n are respectively obtained from the slope and intercept of the $ln(A - \sigma) - ln\,\varepsilon$, that the curve is shown in Figure (6). These values for alloys are reported in table (3). The increase in nickel content in the alloy significantly increased the power of strain hardening and strain hardening coefficient as well, resulting in an increase in flow stress at all temperatures and strain rates for the new alloys in comparison with the base alloy.

At reference temperature, the Eq. (1) can be rewritten as Eq. (3), upon which the slop of the $\frac{\sigma}{A+B\varepsilon^n} - ln\dot{\varepsilon}^*$ curve is the C, which is plotted in Figure (7), and the results are presented in table (4). The coefficient of strain rate hardening is decreased with increasing Ni content in the alloy composition, which may indicate a decrease in the sensitivity of the flow stress to the strain rate for the alloys containing high amounts of nickel.

$$\frac{\sigma}{A + B\varepsilon^n} = 1 + C \ln\dot{\varepsilon}^* \tag{3}$$

In the conditions of the reference strain rate, Eq. (1) converts to Eq. (4). The value of m is obtained from the slope of the $ln\left[1 - \frac{\sigma}{A+B\varepsilon^n}\right] - ln\,T^*$ curve at the reference strain rate and various temperatures, according to Figure (7). The value of m for the alloys is reported in Table (5).
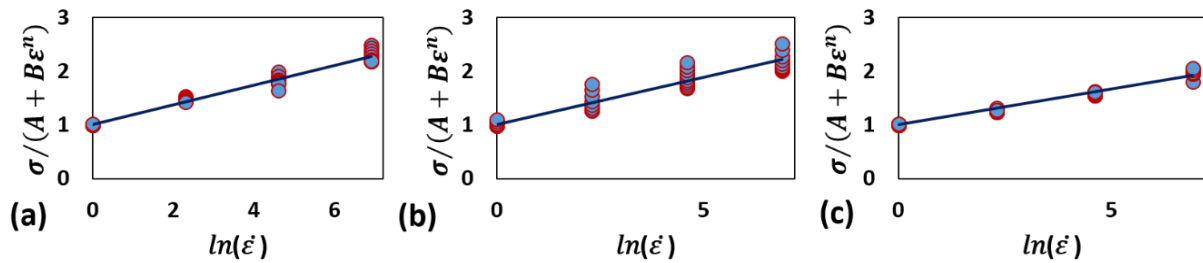
$$\frac{\sigma}{A + B\varepsilon^n} = 1 - T^{*m} \tag{4}$$

Figure 7 The curve of $\frac{\sigma}{A+B\varepsilon^n} - ln\dot{\varepsilon}^*$: a) 0.8% Ni, b) 2% Ni and c) 2.6% Ni.

Table 5 The m values for alloys with different weight percentages of nickel

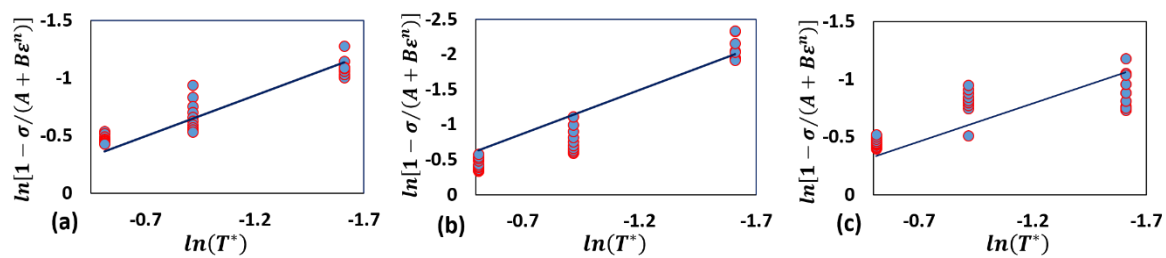| Alloy	m
Al-Si-0.8% Ni	0.7071
Al-Si-2% Ni	1.2422
Al-Si-2.6% Ni	0.6563

Figure 8 The curve of $ln\left[1 - \frac{\sigma}{A+B\varepsilon^n}\right] - ln\,T^*$: a) 0.8% Ni, b) 2% Ni and c) 2.6% Ni.

Table 6 The standard Johnson-Cooke model for alloys with different weight percentages of nickel

Alloy	Johnson-Cooke model
Al-Si-0.8% Ni	$\sigma = (39.42632 - 0.86011\varepsilon^{0.0713})(1 + 0.1844\ln\dot{\varepsilon})(1 - T^{*0.7071})$
Al-Si-2% Ni	$\sigma = (69.43 - 42.6233\varepsilon^{0.8288})(1 + 0.1768\,ln\dot{\varepsilon})(1 - T^{*1.2422})$
Al-Si-2.6% Ni	$\sigma = (75.36155 - 24.4909\varepsilon^{0.7015})(1 + 0.1331\,ln\dot{\varepsilon})(1 - T^{*0.6563})$

Finally, after obtaining all the constants for all three alloys standard Johnson-Cooke is obtained as shown in table (6).

3.2   Modified Johnson-Cook (JC) model

Modified Johnson-Cook (MJC) model was developed based on the Eq. (1). The modified version of the JC model includes both yield and strain hardening and also the effect of strain rate and temperature on the flow behavior, as follows:

$$\sigma = (A + B_1\varepsilon + B_2\varepsilon^2)(1 + C_1 \ln\dot{\varepsilon}^*)exp[(\lambda_2 + \lambda_1 \ln\dot{\varepsilon}^*)(T - T_r)] \tag{5}$$

The calculation process for constants is similar to the standard model, which is briefly described in the previous section. In the reference deformation condition, the Eq. (5) is changed to Eq. (6):

$$\sigma = A + B_1\varepsilon + B_2\varepsilon^2 \tag{6}$$

By plotting the true stress-true strain at the reference strain rate and temperature, and fitting a second-order curve on it, constants A, B_1, and B_2 are calculated that the results are presented in table (7).
In the reference temperature, the modified form of the JC is summarized as follows:

$$\frac{\sigma}{(A_1 + B_1\varepsilon + B_2\varepsilon^2)} = 1 + C_1 \ln\dot{\varepsilon}^* \tag{7}$$

Since the parameters A, B1, and B2 have already been calculated, C_1 is the slope of the fitted line with Intercept equal to 1 on the $ln(\frac{\sigma}{(A_1+B_1\varepsilon+B_2\varepsilon^2)}) - ln\dot{\varepsilon}^*$ data. The $ln(\frac{\sigma}{(A_1+B_1\varepsilon+B_2\varepsilon^2)}) - ln\dot{\varepsilon}^*$ data and the fitted line are shown in Figure (9), and the results are summarized in table (8).
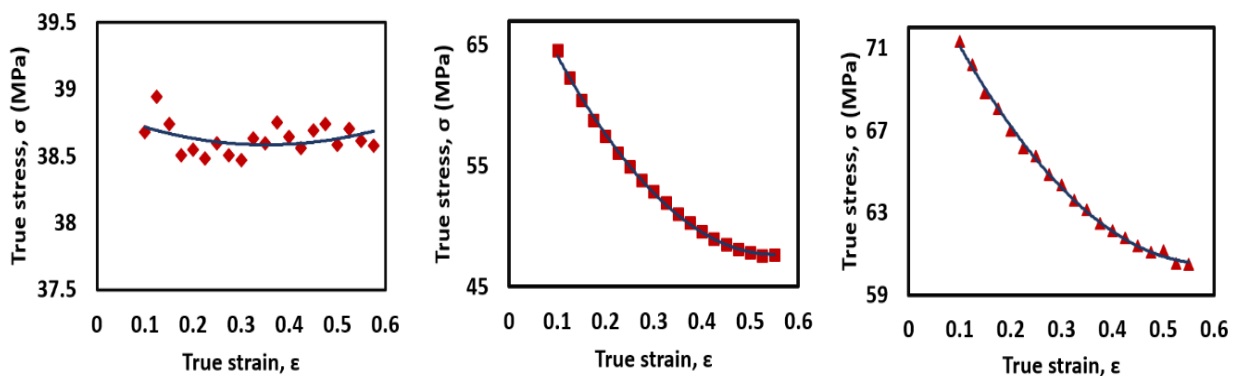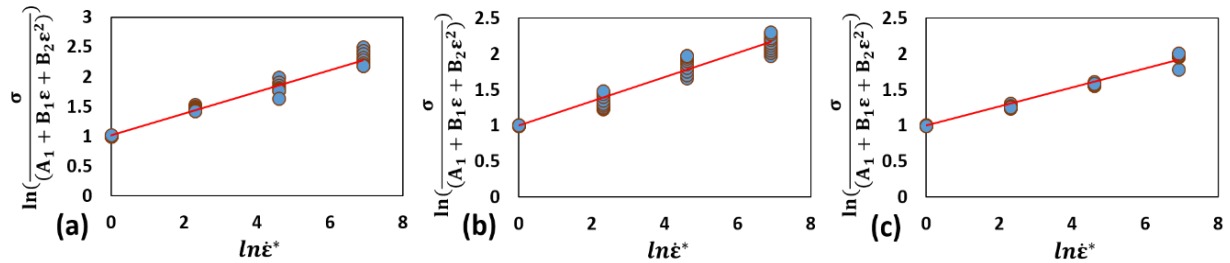

Figure 9 Relationship between ε and σ at the temperature of 673 K and strain rate of 0.001s^{-1} for different Piston alloys

Table 7 The value of A, B1, and B2 for different Piston alloys

Piston Alloy	A	B_1	B_2
Alloy A	38.8	-1.54	2.25
Alloy B	71.86	-86.51	76.72
Alloy C	75.6	-50.15	41.04

Table 8 The value of C_1 for different Piston alloys

Alloy	C_1
Al-Si-0.8% Ni	0.18
Al-Si-2% Ni	0.17
Al-Si-2.6% Ni	0.13

Figure 10 The curve of $ln(\frac{\sigma}{(A_1+B_1\varepsilon+B_2\varepsilon^2)}) - ln\dot{\varepsilon}^*$: a) 0.8%Ni, b)2%Ni and c) 2.6%Ni.

If the new parameter λ, is defined as $\lambda = \lambda_2 + \lambda_1\, ln\dot{\varepsilon}^*$, Eq. (5) can be rewritten as follows:

$$\sigma = (A + B_1\varepsilon + B_2\varepsilon^2)(1 + C_1\, ln\dot{\varepsilon}^*)exp[\lambda(T - T_r)] \qquad (8)$$

The value of the parameter λ for each strain rate is calculated by plotting the $ln[\sigma/(A_1 + B_1\varepsilon + B_2\varepsilon^2)] - (T - T_r)$ data and matching the straight line on them, in which case the value of λ is equal to the slope of the line. Table (9) lists the obtained values of λ for different strain rates. Based on how the parameter λ is adjusted, if the line is fitted on the $\lambda - ln(\dot{\varepsilon}^*)$ points, the slope, and intercept of the line are the value of λ_1 and λ_2 respectively. Figure (10) shows the relation between $\lambda - ln(\dot{\varepsilon}^*)$, and the amount of λ_1 and λ_2 are presented in table (10) for the different alloy.

Table 9 The value of λ under different strain rate for different Piston Alloy

	Strain rate (s^{-1})	0.001	0.01	0.1	1
Al-Si-0.8% Ni		-0.0069	-0.0054	-0.0045	-0.0042
Al-Si-2% Ni	λ	-0.0069	-0.0061	-0.0059	-0.0048
Al-Si-2.6% Ni		-0.0068	-0.0062	-0.0055	-0.0043

Table 10 The value of λ1 and λ2 for different Piston alloy

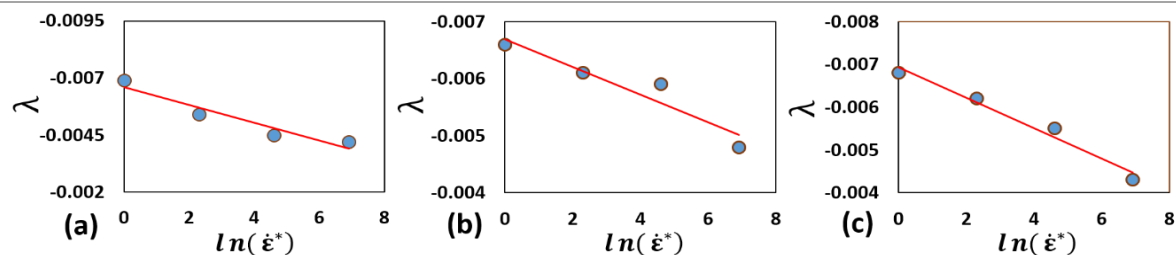| Alloy	λ_1	λ_2
Al-Si-0.8% Ni	-0.0066	0.0004
Al-Si-2% Ni	-0.0067	0.0002
Al-Si-2.6% Ni	-0.0069	0.0004

Figure 11 The curve of $\lambda - ln(\dot{\varepsilon}^*)$: a) 0.8%Ni, b) 2%Ni and c) 2.6%Ni.

Table 11 The modified Johnson-Cooke model for alloys with different weight percentages of nickel

Alloy	Modified Johnson-Cooke model
Al-Si-0.8% Ni	$\sigma = (38.842 - 1.5431\varepsilon + 2.2456\varepsilon^2)(1 + 0.1845\ln\varepsilon^{\cdot*})\exp[(0.0004\ln\varepsilon^{\cdot*} - 0.0066)(T - T_r)]$
Al-Si-2% Ni	$\sigma = (71.857 - 86.509 + 76.72\varepsilon^2)(1 + 0.1697\ln\varepsilon^{\cdot*})\exp[(0.0002\ln\varepsilon^{\cdot*} - 0.0067)(T - T_r)]$
Al-Si-2.6% Ni	$\sigma = (75.596 - 50.147\varepsilon + 41.043\varepsilon^2)(1 + 0.133\ln\varepsilon^{\cdot*})\exp[(0.0004\ln\varepsilon^{\cdot*} - 0.0069)(T - T_r)]$

The final constitutive equation obtained for each of the alloys is presented in table (11).
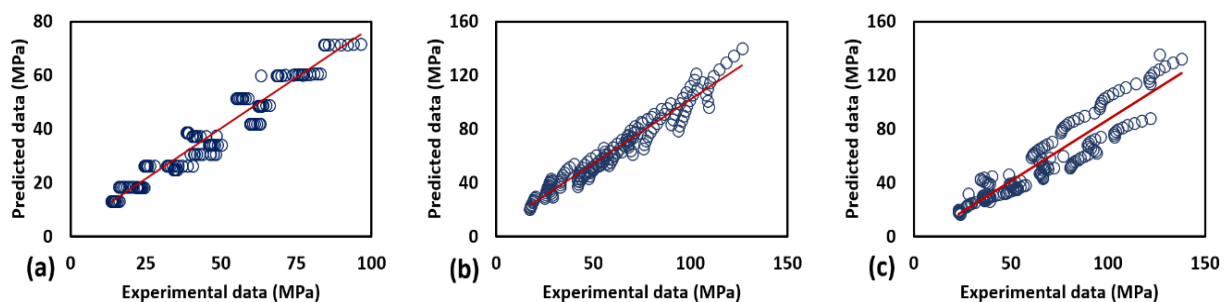
3.3 Accuracy investigation of extracted models

In the investigated strain range, the obtained models are examined in terms of accuracy. For this purpose, conventional statistical methods have been used, and two parameters included the correlation coefficient, and average absolute relative error (AARE) have been used to evaluate the accuracy of the models numerically. The results of this analysis are based on the data which are plotted in Figure (11), and Figure (12) are presented in table (12). The modified model clearly had higher accuracy and was able to predict the flow stress by about 50% more accuracy than the original model. Also the correlation coefficient, R which indicates that how the predicted values are in agreement with the measured values show that both models have been able to predict the changes of the flow stress with acceptable accuracy and the modified model is quite successful in predicting the trends of changes.

From the comparison of the calculated values by the proposed models and measured by the experiments (which are plotted for alloy B in Figure (14) and Figure (15) as examples) It is found that the extracted models are in good agreement with the test values and also the accuracy of the modified model is better in predicting the flow stress, and in particular this model has the ability to predict the trend of stress variation as well. In general, the original model can only predict the hardening or softening process, which can be due to assuming the effects of thermal softening, strain hardening, and strain rate hardening independent.

Table 12 The results of the accuracy studying of the proposed models.

Model	Alloy type (%Wt Ni)	Correlation Coefficient, R	AARE%
Johnson-Cook	Type A (0.8% Ni)	0.97	17
	Type B (2% Ni)	0.97	13
	Type C (2.6% Ni)	0.94	18
Modified Johnson-Cook	Type A (0.8% Ni)	0.99	6
	Type B (2% Ni)	0.98	8
	Type C (2.6% Ni)	0.97	10

Figure 12 The comparison curve of the flow stress calculated by JC model with experiments: a) alloy type A, b) alloy type B, alloy type C.
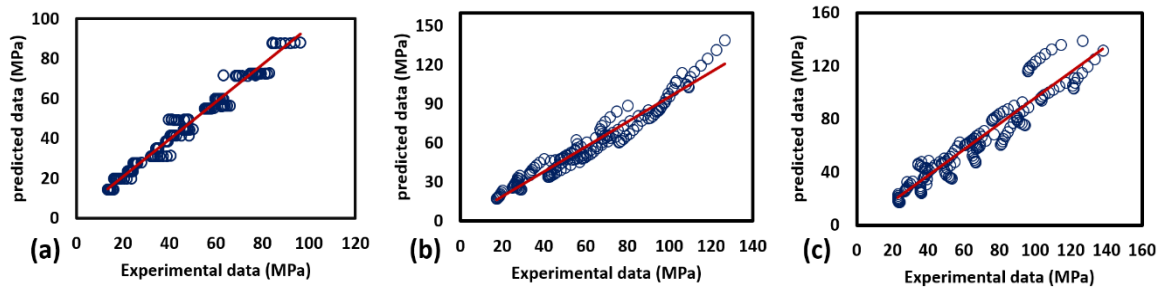
Figure 13 The comparison curve of the flow stress calculated by modified JC model with experiments: a) alloy type A, b) alloy type B, alloy type C.
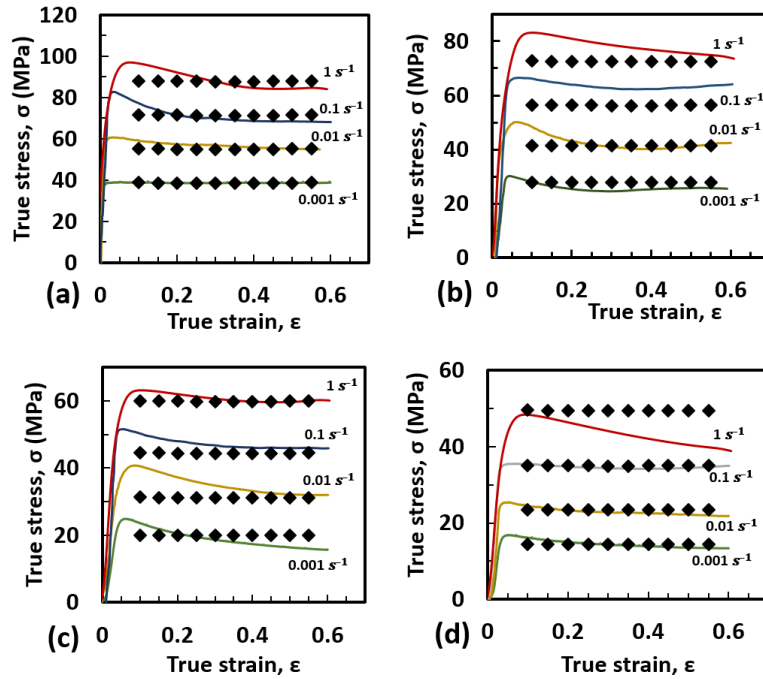

Figure 14 The Comparison of the trend of flow stress calculated by the JC model and the experiment for the alloy type B: a) 673K, b) 723K, c) 773K and d) 823K.
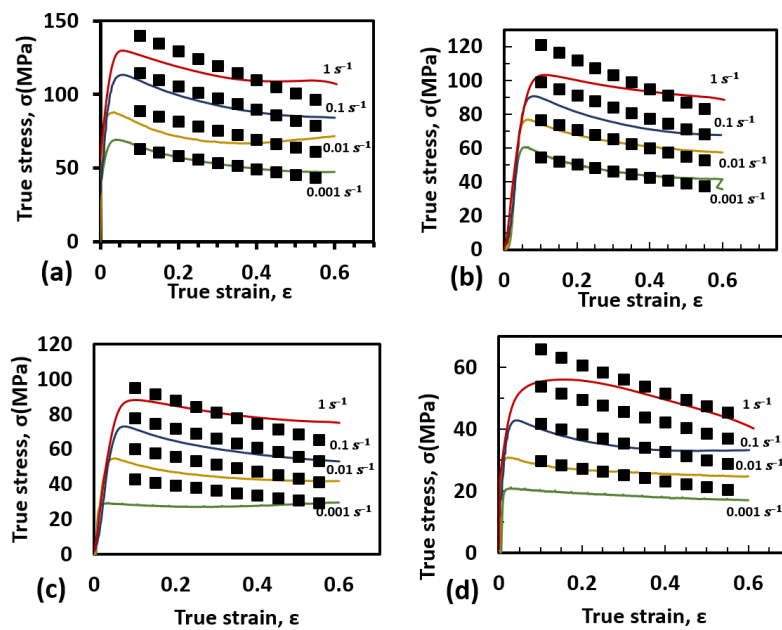

Figure 15 The Comparison of the trend of flow stress calculated by the modified JC model and the experiment for the alloy type B: a) 673K, b) 723K, c) 773K and d) 823K.

4   Conclusions

In this study, the hot deformation process of new alloys of aluminum that made by adding different amounts of nickel to the base aluminum piston alloy was studied to drive new set of constitutive equations based on the Johnson-Cook model which can describe the behavior of these materials under hot deformation conditions. The behavior of all the alloys during deformation was significantly dependent on temperature and strain rate changes. Increasing temperature and strain rate had the opposite effects, and reducing and increasing the flow stress, respectively. The addition of nickel to the base alloy composition has increased its strength and yield stress. Also, by examining the changes of coefficients of the Johnson-Cook equation the susceptibility of the flow stress of the alloys to increase the temperature and strain rate is reduced for the alloys with higher percentages of nickel. The extracted original Johnson-Cook model accurately predicted material behavior with a maximum error of less than 18%, although it did not succeed in predicting the trend of changes in flow stress. This model is particularly inaccurate at high temperature and strain rates, which may be due to its inability of the model to account the combined effects of temperature and strain rate. The use of the modified model has significantly increased accuracy and increased it to about twice for each alloy. The modified model has also been able to predict the trend of changes in flow stress, and also has been able to predict the recovery or hardening process on the data during deformation.

References

[1] Polmear, I., StJohn, D., Nie, J-F., and Qian, M., "*Light Alloys: Metallurgy of the Light Metals*", 5th Edition, Butterworth-Heinemann, Australia, pp. 544, (2017).

[2] Davis, J.R., "*Aluminum and Aluminum Alloys*", ASM International, Metal Park, Ohio, pp. 784, (1993).

[3] Hoag, K., and Dondlinger, B., "*Vehicular Engine Design*", 2nd Edition, Springer Vienna, pp. 227, (2015).

[4] Committee, A.I.H., "*Properties and Selection: Nonferrous Alloys and Special-purpose Materials*", ASM International, Metal Park, Ohio, Vol. 2, pp. 1143-1144, (1992).

[5] Lin, Y.C., Li, Q-F., Xia, Y.C., and Li, L-T., "A Phenomenological Constitutive Model for High Temperature Flow Stress Prediction of Al–Cu–Mg Alloy", Materials Science and Engineering: A, Vol. 534, pp. 654-662, (2012).

[6] Stadler, F., Antrekowitsch, H., Frangner, W., Kaufmann, H., and Uggowitzer, P.J., "Effect of Main Alloying Elements on Strength of Al–Si Foundry Alloys at Elevated Temperatures", International Journal of Cast Metals Research, Vol. 25, pp. 215-224, (2012).

[7] Mirzaee-Moghadam, M., Lashgari, H.R., Zangeneh, Sh., Rasaee, S., Seyfor, M., Asnavandi, M., and Mojtahedi, M., "Dry Sliding Wear Characteristics, Corrosion Behavior, and Hot Deformation Properties of Eutectic Al–Si Piston Alloy Containing Ni-rich Intermetallic Compounds", Materials Chemistry and Physics, Vol. 279, Article Number: 125758, https://doi.org/10.1016/j.matchemphys.2022.125758, (2022).

[8] Johnson, G.R., "A Constitutive Model and Data for Materials Subjected to Large Strains, High Strain Rates, and High Temperatures", Proceedings 7th International Symposium on Ballistics, The Hague, Netherlands, April 19-21, pp. 541-547, (1983).

[9] Abbasi-Bani, A., Zarei-Hanzaki, A., Pishbin, M.H., and Haghdadi, N., "A Comparative Study on the Capability of Johnson–Cook and Arrhenius-type Constitutive Equations to Describe the Flow Behavior of Mg–6Al–1Zn Alloy", Mechanics of Materials, Vol. 71, pp. 52-61, (2014).

[10] Immanuel, R., and Panigrahi, S., "Deformation Behavior of Ultrafine Grained A356 Material Processed by Cryorolling and Development of Johnson–Cook Model", Materials Science and Engineering: A, Vol. 712, pp. 747-756, (2018).

[11] He, A., Xie, G., Zhang, H., and Wang, X., "A Comparative Study on Johnson–Cook, Modified Johnson–Cook and Arrhenius-type Constitutive Models to Predict the High Temperature Flow Stress in 20CrMo Alloy Steel", Materials and Design, Vol. 52, pp. 677-685, (2013).

[12] Lin, Y., and Chen, X-M., "A Combined Johnson–Cook and Zerilli–armstrong Model for Hot Compressed Typical High-strength Alloy Steel", Computational Materials Science, Vol. 49, pp. 628-633, (2010).

[13] Lin, Y., Chen, X.-M., and Liu, G., "A Modified Johnson–Cook Model for Tensile Behaviors of Typical High-strength Alloy Steel", Materials Science and Engineering: A, Vol. 527, pp. 6980-6986, (2010).

[14] Li, H-Y., Wang, X-F., Duan, J-Y., and Liu, J-J., "A Modified Johnson Cook Model for Elevated Temperature Flow Behavior of T24 Steel", Materials Science and Engineering: A, Vol. 577, pp. 138-146, (2013).

[15] Samantaray, D., Mandal, S., and Bhaduri, A., "A Comparative Study on Johnson Cook, Modified Zerilli–Armstrong and Arrhenius-type Constitutive Models to Predict Elevated Temperature Flow Behaviour in Modified 9Cr–1Mo Steel", Computational Materials Science,Vol. 47, pp. 568-576, (2009).

[16] Hou, Q.Y., and Wang, J.T., "A Modified Johnson–Cook Constitutive Model For Mg–Gd–Y Alloy Extended to a Wide Range of Temperatures", Computational Materials Science, Vol. 50, pp. 147-152, (2010).

[17] Chen, L., Zhao, G., and Yu, J., "Hot Deformation Behavior and Constitutive Modeling of Homogenized 6026 Aluminum Alloy", Materials and Design, Vol. 74, pp. 25-35, (2015).

[18] Rasaee, S., and Mirzaei, A., "Constitutive Modeling of 2024 Aluminum Alloy Based on the Johnson–Cook Model", Transactions of the Indian Institute of Metals, Vol. 72, pp. 1023-1030, (2019).

[19] Committee, A., "*Heat Treating*", ASM Handbook, International Library Service, Utah, Vol. 4, pp. 420-424, (1991).

[20] Prasad, Y., Rao, K., and Sasidhar, S., "*Hot Working Guide: a Compendium of Processing Maps*", ASM International, Materials Park, Ohio, pp. 545, (2015).

Nomenclature

σ	Flow stress
ε	Strain
T	Temperature
$\dot{\varepsilon}$	Strain rate
$\dot{\varepsilon}^*$	Dimensionless strain rate $\dot{\varepsilon}^* = \dot{\varepsilon}/\dot{\varepsilon}_r$
T^*	Homologous temperature: $T^* = (T - T_r)/(T_m - T_r)$
T_r	The temperature at the reference condition: $T_r = 673\ K$
$\dot{\varepsilon}_r$	The strain rate at the reference condition: $\dot{\varepsilon}_r = 0.001\ s^{-1}$.
A	The yield stress of the alloy at a reference condition
n	The strain hardening coefficient
B	The power of strain hardening

Table captions

Table (1) The chemical composition of the alloys
Table (2) The A values for alloys with different weight percentages of nickel
Table (3) The n and B values for alloys with different weight percentages of nickel
Table (4) The C values for alloys with different weight percentages of nickel
Table (5) The m values for alloys with different weight percentages of nickel
Table (6) The standard Johnson-Cooke model for alloys with different weight percentages of nickel
Table (7) The value of A, B1, and B2 for different Piston alloys
Table (8) The value of C_1 for different Piston alloys
Table (9) The value of λ under different strain rate for different Piston Alloy
Table (10) The value of λ1 and λ2 for different Piston alloy
Table (11) The modified Johnson-Cooke model for alloys with different weight percentages of nickel
Table (12) The results of the accuracy studying of the proposed models.

Figure captions

Figure (1) The cylindrical samples for high-temperature compression test.   45
Figure (2) The initial microstructure of the alloys: a) Al-Si-0.8% Ni, b) Al-Si-2% Ni, c) Al-Si-2.6% Ni.
Figure (3) The true stress–strain curves of Al-Si-0.8% Ni with various strain rates and at the deformation temperatures of a) 673K, b) 723K, c) 773K and d) 823K.
Figure (4) The true stress–strain curves of Al-Si-2% Ni with various strain rates and at the deformation temperatures of a) 673K, b) 723K, c) 773K and d) 823K.
Figure (5) The true stress–strain curves of Al-Si-2.6% Ni with various strain rates and at the deformation temperatures of a) 673K, b) 723K, c) 773K and d) 823K.
Figure (6) The curve of $ln(A - σ) - ln\ \varepsilon$: a) 0.8%Ni, b)2%Ni, and c) 2.6%Ni.

Figure (7) The curve of $\frac{\sigma}{A+B\varepsilon^n} - ln\dot{\varepsilon}^*$: a) 0.8%Ni, b)2%Ni and c) 2.6%Ni.

Figure (8) The curve of $ln\left[1 - \frac{\sigma}{A+B\varepsilon^n}\right] - ln\,T^*$: a) 0.8%Ni, b)2%Ni and c) 2.6%Ni.

Figure (9) Relationship between ε and σ at the temperature of 673 K and strain rate of 0.001s⁻¹ for different Piston alloys

Figure (10) The curve of $ln(\frac{\sigma}{(A_1+B_1\varepsilon+B_2\varepsilon^2)}) - ln\dot{\varepsilon}^*$: a) 0.8%Ni, b)2%Ni and c) 2.6%Ni.

Figure (11) The curve of $\lambda - ln(\dot{\varepsilon}^*)$: a) 0.8%Ni, b)2%Ni and c) 2.6%Ni.

Figure (12) The comparison curve of the flow stress calculated by JC model with experiments: a) alloy type A, b) alloy type B, alloy type C.

Figure (13) The comparison curve of the flow stress calculated by modified JC model with experiments: a) alloy type A, b) alloy type B, alloy type C.

Figure (14) Comparison of the trend of flow stress calculated by the JC model and the experiment for the alloy type B: a) 673K, b) 723K, c) 773K and d) 823K.

Figure (15) Comparison of the trend of flow stress calculated by the modified JC model and the experiment for the alloy type B: a) 673K, b) 723K, c) 773K and d) 823K.